PAPER

CrossMark
click for updates

Ru−B nanoparticles on metal−organic frameworks as excellent catalysts for hydrogenation of benzene to cyclohexane under mild reaction conditions†

Huizi Bi,‡[a] Xiaohe Tan,‡[a] Rongfei Dou,[a] Yan Pei,[a] Minghua Qiao,*[a] Bin Sun[b] and Baoning Zong*[b]

The ever-increasing industrial demands for nylon-6 and nylon-66 and the more and more stringent regulations on particulate emission in exhaust gases necessitate the development of an energy-efficient and environment-friendly method for saturation hydrogenation of benzene and its derivatives. However, the hydrogenation of benzene is usually conducted at a high temperature and/or under high H_2 pressure, which is energy-consuming and of low environmental safety. Here, we prepared amorphous Ru−B/MIL-53(Al, Cr, and AlCr) catalysts *via* the wetness impregnation−chemical reduction method, which were comprehensively characterized by a combination of techniques. We found that the Ru−B/MIL-53 catalysts could catalyse the hydrogenation of benzene to cyclohexane under mild reaction conditions of 30 °C and 1.0 MPa of H_2 with high efficiency, among which the Ru−B/MIL-53(AlCr) catalyst exhibited the highest turnover frequency (TOF) in terms of benzene of 6.4 s^{-1}. Moreover, this catalyst showed good recyclability and high activities in the hydrogenation of toluene, *o*-xylene, *m*-xylene, *p*-xylene, and mesitylene as well, which shows promise for the application of the Ru−B/MIL-53 catalysts in the industrially important and environmentally desirable hydrogenation reaction of benzene and its derivatives.

Introduction

The catalytic hydrogenation of benzene is essential for cyclohexane manufacture and transportation fuel upgrading. Cyclohexane is widely used in the synthesis of fine chemicals and intermediates including cyclohexanol, cyclohexanone, caprolactam, hexamethylenediamine, adipic acid, and so on.[1] It is also an excellent solvent comparable to benzene for resins, tars, and cellulose ethers but of far lower toxicity.[2] On the other hand, depletion of benzene and other aromatics in transportation fuels by hydrogenation is critical for diminishing the emission of particulate matters in exhaust gases and increasing the cetane number of diesel fuel.[3,4]

In industry, the hydrogenation of benzene is conducted at a high temperature (≥100 °C) and/or under high H_2 pressure (≥5 MPa) over group VIII metals to facilitate its high-efficiency conversion.[5] There have been many endeavours in the development of unsupported catalysts and catalysts supported on SiO_2, Al_2O_3, zeolite, SBA-15, and carbon nanotubes (CNTs) for this reaction under mild reaction conditions (ESI, Table S1†). The highest TOF of 1.5 s^{-1} was reported on the NFS-Ru(0) catalyst with ruthenium(0) nanoclusters stabilized by a nanozeolite-Y at 25 °C and 42 psig of H_2.[6] Although the TOF of the Ru/CNT catalyst is apparently higher than that of NFS-Ru(0), it should be mentioned that the activity of the former was obtained at much higher temperature (80 °C) and H_2 pressure (4 MPa).[7]

Recently, metal–organic frameworks (MOFs) have aroused great interest in fields including catalysis,[8,9] drug delivery,[10] gas separation,[11] and gas storage.[12] Desirably, the high surface area of the MOFs is anticipated to guarantee high metal dispersion, which has practical benefit to the catalytic activity. Hence, some efforts, yet limited, have been devoted to the synthesis of MOF-supported Ru catalysts for the hydrogenation of benzene to cyclohexane. Schröder *et al.* prepared the Ru@MOF-5 catalyst by gas-phase deposition of volatile [Ru(cod)(cot)] (cod = 1,5-cyclooctadiene, cot = 1,3,5-cyclooctatriene)

[a]*Collaborative Innovation Center of Chemistry for Energy Materials, Department of Chemistry and Shanghai Key Laboratory of Molecular Catalysis and Innovative Materials, Fudan University, Shanghai 200433, P. R. China.*
E-mail: mhqiao@fudan.edu.cn
[b]*State Key Laboratory of Catalytic Materials and Chemical Engineering, Research Institute of Petroleum Processing, SINOPEC, Beijing 100083, P. R. China.*
E-mail: zongbn.ripp@sinopec.com
†Electronic supplementary information (ESI) available. See DOI: 10.1039/c5gc02683k
‡They contributed equally to this work.

into MOF-5 followed by hydrogenolysis,[13] on which the conversion of benzene was 20% under relatively mild reaction conditions (75 °C, 3 bar H_2) for 20 h. Zhao et al. prepared the Ru/La-MOF catalyst using $RuCl_3·3H_2O$ as the metal precursor in CO_2–methanol supercritical fluid (SCF) at 200 °C.[14] Under the reaction conditions of 60 °C and 6 MPa of H_2, benzene was completely converted to cyclohexane in 2 h with the TOF of 0.69 s^{-1}, which is substantially higher than the TOF of 0.18 s^{-1} over a commercial Ru/C catalyst. Liu et al. prepared the bimetallic Ru–Pt/MIL-101 catalyst using the colloidal deposition method, on which the TOF of 0.71 s^{-1} was reported at 60 °C and 1 MPa of H_2.[15] However, these MOF-supported Ru catalysts suffer from drawbacks of sophisticated preparation procedures, low activity, or high pressure for the reaction. To develop highly active, easy to prepare, and reusable benzene hydrogenation catalysts that are suitable for mild reaction conditions is therefore of great academic and industrial significance.

In this work, we synthesized MIL-53(Al), MIL-53(Cr), and MIL-53(AlCr) MOFs as supports first, followed by depositing amorphous Ru–B nanoparticles (NPs) on them by the facile wetness impregnation–chemical reduction method (see the ESI† for detailed preparation procedures). MIL-53(Al) and MIL-53(Cr) belong to the subfamily of MOFs synthesized and named by Férey and coworkers with MIL standing for Materials Institute of Lavoisier.[16,17] MIL-53 is built up from infinite corner-sharing octahedral $MO_4(OH)_2$ (M = trivalent metal cation) chains linked to each other three-dimensionally through the 1,4-benzenedicarboxylic acid (H_2BDC) molecules. The MIL-53(Al) and MIL-53(Cr) MOFs were exploited in this work as the supports mainly owing to the distinctive structural stability of MIL-53,[16,17] which is a key character for catalytic applications. For this reason, we analogously synthesized a novel MIL-53(AlCr) MOF with Al^{3+} and Cr^{3+} coordination cations coexisting in this material. We found that the MIL-53 MOFs are excellent supports for the Ru–B NPs to catalyse the hydrogenation of benzene to cyclohexane under mild reaction conditions of 30 °C and 1.0 MPa of H_2.

Results and discussion

Table S2† compiles the physicochemical properties of the MIL-53 supports and the corresponding Ru–B/MIL-53 catalysts. By inductively coupled plasma-atomic emission spectroscopy (ICP–AES), we identified that the practical loadings of Ru on all three Ru–B/MIL-53 catalysts were close to the nominal loading of 8.0 wt%, showing that the wetness impregnation–chemical reduction method is effective in quantitatively depositing the metal on the MIL-53 supports. As expected, the Brunauer–Emmett–Teller surface area (S_{BET}) and the pore volume (V_p) of the Ru–B/MIL-53 catalysts were reduced compared to those of the MIL-53 counterparts, while the average pore size (d_p) remained unchanged after the deposition of Ru–B. The lowest decrease in the S_{BET} was found on Ru–B/MIL-53(AlCr), implying the highest dispersion of the Ru–B NPs on MIL-53

(AlCr) irrespective of the lowest S_{BET} of MIL-53(AlCr). This is in agreement with the higher active surface area (S_{Ru}) of Ru–B/MIL-53(AlCr) (17 m^2 g$_{Ru}^{-1}$) than those of Ru–B/MIL-53(Al) (10 m^2 g$_{Ru}^{-1}$) and Ru–B/MIL-53(Cr) (15 m^2 g$_{Ru}^{-1}$) determined by pulsed adsorption of CO.

Fig. 1a shows that the X-ray diffraction (XRD) patterns of the as-synthesized MIL-53(Al) and MIL-53(Cr) matched well with those previously reported in terms of diffraction angles and relative intensities.[16,17] Although the diffractogram of the novel MIL-53(AlCr) is not available in the literature, a direct comparison with those of MIL-53(Al) and MIL-53(Cr) verifies that MIL-53(AlCr) bears an identical crystallographic structure. In addition, the intensities of the diffraction peaks of MIL-53(AlCr) were in-between those of MIL-53(Al) and MIL-53(Cr), inferring that MIL-53(AlCr) contains both the coordinative metal cations. This is further confirmed by chemical analysis that Al and Cr coexist in MIL-53(AlCr) with an Al : Cr atomic ratio of 0.7 : 1, which is lower than the nominal ratio of 1 : 1. During the synthesis of MIL-53(AlCr), we added HF by referring to the synthesis protocol of MIL-53(Cr), which might be adverse to the thorough coordination of the Al cations with H_2BDC.

As for the Ru–B/MIL-53 catalysts, Fig. 1b demonstrates that the diffractograms of the MIL-53 supports remained intact, confirming that depositing the Ru–B NPs by the wetness impregnation–chemical reduction method did not disturb their lattice frameworks. Besides, there was a vague and broad
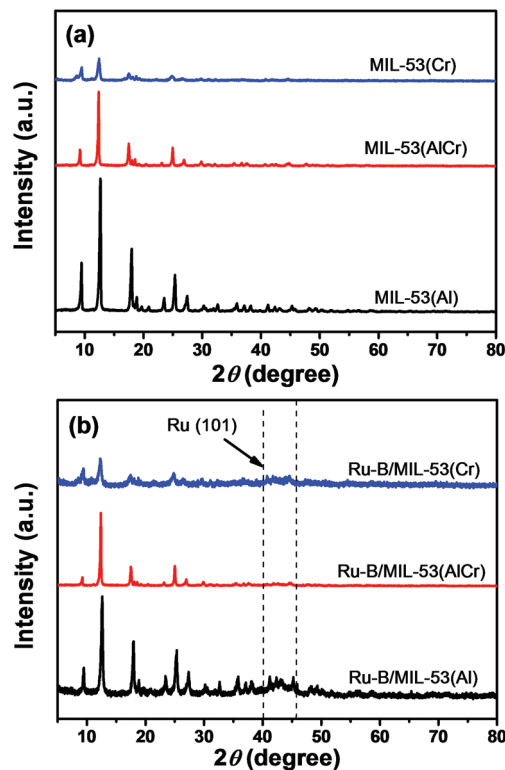

Fig. 1 XRD patterns of (a) the MIL-53(Al), MIL-53(AlCr), and MIL-53(Cr) supports, and (b) the corresponding Ru–B/MIL-53 catalysts.

peak at 2θ of *ca.* 43° for these catalysts, which is attributable to the formation of the Ru–B NPs with an amorphous structure.[18]

Fig. 2 presents the transmission electron microscopy (TEM) images of the Ru–B/MIL-53 catalysts and the particle size distribution (PSD) histograms of the Ru–B NPs. The MIL-53 supports were decorated with highly dispersed Ru–B NPs with the mean diameters of 3.7 ± 0.7, 3.7 ± 0.8, and 3.2 ± 0.4 nm on MIL-53(Al), MIL-53(Cr), and MIL-53(AlCr), respectively. The selected-area electron diffraction (SAED) patterns acquired on the Ru–B NPs only give rise to a diffraction halo rather than distinct dots (insets in Fig. 2), further corroborating the amorphous structure of the Ru–B NPs.[19]

Fig. 3 shows the Fourier transform infrared (FTIR) spectra of the MIL-53 supports and the Ru–B/MIL-53 catalysts. The carboxyl groups in the free H_2BDC molecule exhibit characteristic asymmetric and symmetric vibration bands at 1678 and 1282 cm^{-1}, respectively.[20,21] For MIL-53(Al), these bands shifted to 1579 and 1413 cm^{-1}, and the corresponding wavenumber difference was 166 cm^{-1}, which is substantially smaller than that of free H_2BDC (396 cm^{-1}) due to coordination with the metal cations.[22] The corresponding bands of MIL-53(Cr) were located at 1535 and 1394 cm^{-1} with the wavenumber difference of 141 cm^{-1},[23] inferring that the Cr cations
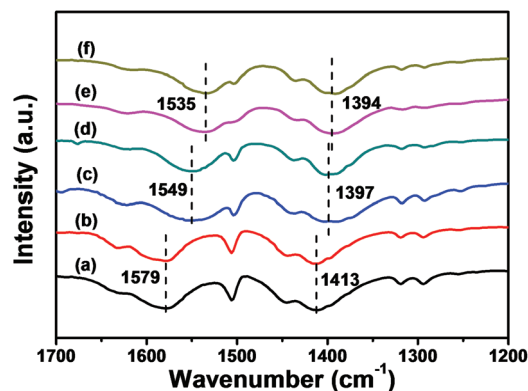

Fig. 3 FTIR spectra of (a) MIL-53(Al), (b) Ru-B/MIL-53(Al), (c) MIL-53(AlCr), (d) Ru-B/MIL-53(AlCr), (e) MIL-53(Cr), and (f) Ru-B/MIL-53(Cr).

coordinate more tightly with H_2BDC than the Al cations. MIL-53(AlCr) showed mediate wavenumbers (1549 and 1397 cm^{-1}) and wavenumber difference (152 cm^{-1}) that are relatively closer to those of MIL-53(Cr). These findings are in line with the fact that MIL-53(AlCr) contains more Cr than Al. The deposition of the Ru–B NPs did not have influence on the vibration frequencies of the carboxyl groups in these MIL-53 supports, which is compatible with the XRD results that the structure of the MIL-53 supports remained intact in the presence of the Ru–B NPs.

Thermogravimetric analysis (TGA) was employed to examine the structural stability of the MIL-53 supports and the Ru–B/MIL-53 catalysts. As shown in Fig. 4, the MIL-53 supports and the catalysts experienced two weight loss stages. The small weight loss below 100 °C is assigned to the desorption of physisorbed water or residual organic solvents. Then, they remained stable up to 514 °C for MIL-53(Al), 374 °C for MIL-53(AlCr), and 328 °C for MIL-53(Cr). The decomposition temperatures of the Ru–B/MIL-53 catalysts were lower than those of the MIL-53 counterparts, indicating that the Ru–B NPs promoted the collapse of the MIL-53 frameworks. Nonetheless, the decomposition temperatures were well above 300 °C even for
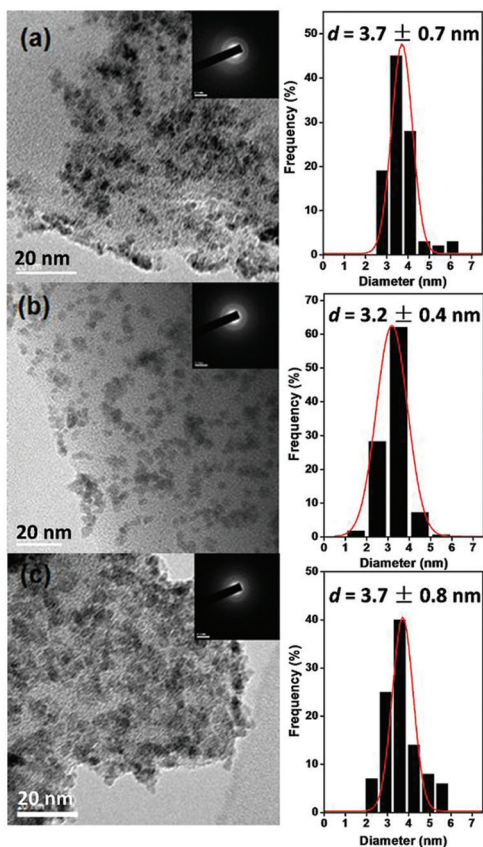

Fig. 2 TEM images and particle size distribution histograms of the (a) Ru–B/MIL-53(Al), (b) Ru–B/MIL-53(AlCr), and (c) Ru–B/MIL-53(Cr) catalysts. Insets are their corresponding SAED patterns.
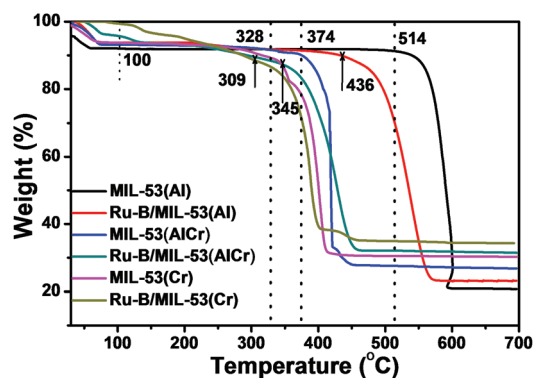

Fig. 4 TGA curves of the MIL-53 supports and the corresponding Ru–B/MIL-53 catalysts.

the least stable Ru–B/MIL-53(Cr), which are sufficient to resist the reaction temperature employed for the hydrogenation of benzene.

Fig. 5 presents the Ru 3p$_{3/2}$ spectra of the Ru–B/MIL-53(Al), Ru–B/MIL-53(Cr), and Ru–B/MIL-53(AlCr) catalysts. These spectra were well fitted by a main peak maximizing at the binding energy (BE) of 461.1 eV and a shoulder peak at a higher BE of 463.2 eV. The former is readily assignable to metallic Ru,[24] while the latter may be related to the formation of Ru–O linkages between the periphery of the Ru–B NPs and the carboxyl groups of H$_2$BDC,[14] which may contribute to the small size and high dispersion of the Ru–B NPs on these MIL-53 supports.

The catalytic results over the Ru–B/MIL-53(Al), Ru–B/MIL-53(Cr), and Ru–B/MIL-53(AlCr) catalysts in the hydrogenation of benzene to cyclohexane under reaction conditions of 30 °C and 1.0 MPa of H$_2$ are summarized in Table 1 as entries 1–3.
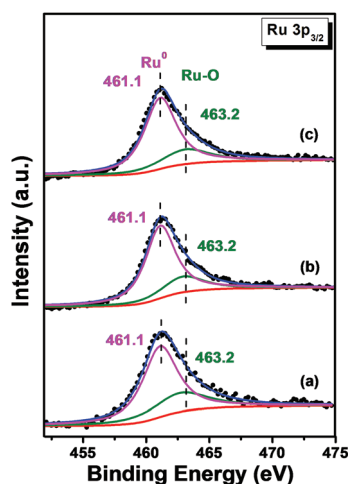

Fig. 5 The Ru 3p spectra of the (a) Ru–B/MIL-53(Al), (b) Ru–B/MIL-53(AlCr), and (c) Ru–B/MIL-53(Cr) catalysts.

Table 1 The hydrogenation results of benzene over the Ru–B/MIL-53 catalysts[a]

Entry	Catalyst	T (°C)	Conv.[b] (%)	r_0[c]	TOF[d] (s^{-1})
1	Ru–B/MIL-53(Al)	30	62	6.4	5.4
2	Ru–B/MIL-53(Cr)	30	80	9.2	5.0
3	Ru–B/MIL-53(AlCr)	30	94	14	6.4
4	Ru–B/MIL-53(AlCr)[e]	30	93	—	—
5	Ru–B/MIL-53(AlCr)[f]	30	94	—	—
6	Ru–B/MIL-53(AlCr)[g]	30	86	—	—
7	Ru–B/MIL-53(AlCr)	20	—	8.0	3.5
8	Ru–B/MIL-53(AlCr)	40	—	24	11

[a] Reaction conditions: 108 mg catalyst, 5.0 ml benzene, 15 ml ethanol, H$_2$ pressure of 1.0 MPa, and stirring rate of 1200 rpm. [b] Measured at reaction time of 1.0 h. [c] Initial weight specific activity, unit in mmol g$_{cat}^{-1}$ min^{-1}. [d] The amount of benzene converted per mole of Ru on the surface per second. [e] The 2nd run. [f] The 3rd run. [g] The 4th run.

In the same time span of 1.0 h, the benzene conversions increased in the following order: 62% < 80% < 94% on Ru–B/MIL-53(Al), Ru–B/MIL-53(Cr), and Ru–B/MIL-53(AlCr), respectively. The initial weight specific hydrogenation rate of benzene (r_0) displayed the same trend. Based on the S_{Ru} and r_0 data, the TOFs of benzene were calculated as 5.4, 5.0, and 6.4 s^{-1} for Ru–B/MIL-53(Al), Ru–B/MIL-53(Cr), and Ru–B/MIL-53(AlCr), respectively. Since the S_{Ru} of Ru–B/MIL-53(Cr) was greater than that of Ru–B/MIL-53(Al), the intrinsic activity of the former was slightly lower than that of the latter. Considering the similar electronic properties of the Ru–B/MIL-53 catalysts (Fig. 5), the enhanced activity of Ru–B/MIL-53(AlCr) may be attributed to the smallest size of the Ru–B NPs on this catalyst (Fig. 2).

Remarkably, the TOFs on all Ru–B/MIL-53 catalysts are nearly one order of magnitude higher than that of the Ru/La-MOF catalyst tested at a higher reaction temperature of 60 °C and H$_2$ pressure of 6 MPa.[14] The intrinsic activities of the Ru–B/MIL-53 catalysts are also higher than those of the inorganic oxide- and CNT-supported Ru catalysts. For instance, Nandanwar et al. reported the TOF of 0.39 s^{-1} on the Ru/γ-Al$_2$O$_3$ nanocatalyst under the reaction conditions of 80 °C and 20 bar of H$_2$.[25] Ma et al. reported the TOF of 1.9 s^{-1} on the Ru/CNT catalyst at 80 °C and 4 MPa of H$_2$.[7] Zahmakıran et al. reported the TOF of 1.5 s^{-1} on the NFS-Ru(0) catalyst at 25 °C and 42 psig of H$_2$.[6] When we lowered the reaction temperature to 20 °C, the TOF over Ru–B/MIL-53(AlCr) (entry 7, Table 1) was still higher than that of NFS-Ru(0); however, one could not make too much about the difference in this case, as NFS-Ru(0) was tested under lower H$_2$ pressure. When the reaction temperature was elevated to 40 °C, the TOF over Ru–B/MIL-53(AlCr) was further increased to as high as 11 s^{-1} (entry 8, Table 1). With the r_0 values in entries 3, 7, and 8 of Table 1, we obtained a linear Arrhenius plot (ESI, Fig. S1†), which gives the apparent activation energy (E_a) of 44 kJ mol^{-1} for the hydrogenation of benzene on Ru–B/MIL-53(AlCr).

In order to confirm that the hydrogenation of benzene on the Ru–B/MIL-53 catalysts is heterogeneous rather than homogeneous, several control experiments were carried out using Ru–B/MIL-53(AlCr) as a representative. After the first catalytic run on Ru–B/MIL-53(AlCr) for 70 min (line a, Fig. 6), no Ru was detected by ICP–AES with the detection limit of ~50 ppb for Ru in the filtrate. In another catalytic run, after 30 min of reaction, the reaction was interrupted, the Ru–B/MIL-53(AlCr) catalyst was separated from the liquid phase by centrifugation, and then the reaction was recommenced in the absence of the catalyst. As anticipated, no noticeable conversion of benzene took place (line b, Fig. 6), which unambiguously manifests the heterogeneity of the reaction as well as the tight binding of the Ru–B NPs on MIL-53(AlCr). Besides, as a blanket reaction, the MIL-53(AlCr) support alone (100 mg) was used as the catalyst in the hydrogenation of benzene under otherwise the same reaction conditions. In this case, no conversion of benzene was detected even by prolonging the reaction time to 5.0 h (line c, Fig. 6), showing that the MIL-53 support itself is inert in the reaction. This finding also evidences that the superior
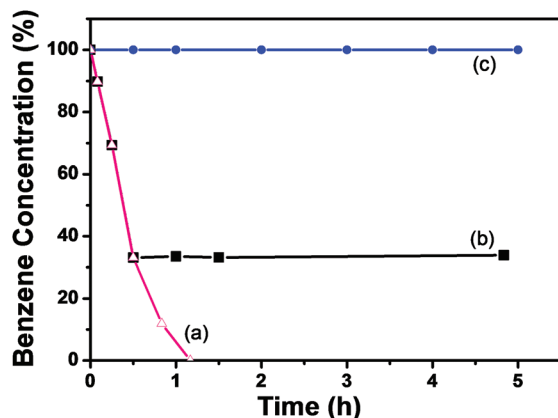
Fig. 6 (a) Plot of the concentration of benzene *versus* time on the Ru−B/MIL-53(AlCr) catalyst, (b) control experiment by removing the catalyst after 30 min of reaction, and (c) control experiment by using MIL-53(AlCr) to catalyse the hydrogenation of benzene. Other reaction conditions are identical to those described in footnote *a* of Table 1.

activity of the Ru−B/MIL-53(AlCr) catalyst is not due to the possible contribution of the MIL-53(AlCr) support in catalysing the reaction.

As an important character of a catalyst, the stability of the Ru−B/MIL-53(AlCr) catalyst was examined. After the reaction went on for 1.0 h, the catalyst was separated by centrifugation, washed three times with ethanol, and reused in a successive run. As shown in entries 3–5 of Table 1, the activity remained virtually unchanged in three runs, which may be associated with the presence of the Ru–O linkages that stabilize the Ru–B NPs. Deactivation was observed at the fourth run, though it still retained 91.3% of its initial activity (entry 6, Table 1). Material loss due to attrition in stirred liquid-phase reaction and repetitive catalyst recovery are common reasons for catalyst deactivation. The slight agglomeration of the Ru–B NPs observed by TEM after the fourth run (Fig. 7a) may also be responsible for catalyst deactivation. Nevertheless, a comparison of the FTIR spectra of the Ru–B/MIL-53(AlCr) catalyst before and after four successive runs in Fig. 7b clearly demonstrates that the characteristic vibration bands of MIL-53(AlCr)
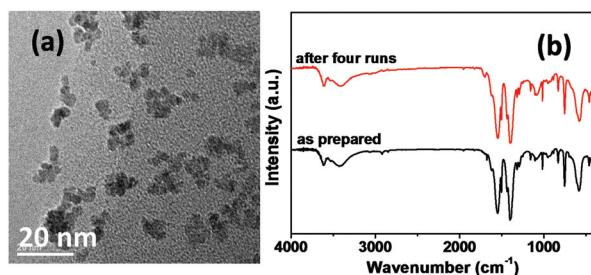

Fig. 7 (a) TEM image of the Ru−B/MIL-53(AlCr) catalyst after four catalytic runs in the hydrogenation of benzene, and (b) a comparison of the FTIR spectra of the Ru−B/MIL-53(AlCr) catalyst before and after four catalytic runs.

Table 2 The hydrogenation results of the methyl-substituted benzene derivatives on the Ru−B/MIL-53(AlCr) catalyst[a]

Substrate	Substrate/Ru (mol/mol)	Conv.[b] (%)	r_0 [c]	TOF[d] (s^{-1})
Toluene	595	53	4.3	2.0
o-Xylene	512	43	2.5	1.2
m-Xylene	512	38	1.2	0.56
p-Xylene	512	31	0.77	0.36
Mesitylene	458	14	0.33	0.15

[a] Reaction conditions: 108 mg Ru–B/MIL-53(AlCr) catalyst, 5.0 ml substrate, 15 ml ethanol, temperature of 30 °C, H_2 pressure of 1.0 MPa, and stirring rate of 1200 rpm. [b] Measured at reaction time of 1.0 h. [c] Initial weight specific activity, unit in mmol g_{cat}^{-1} min^{-1}. [d] The amount of substrate converted per mole of Ru on the surface per second.

are essentially identical, verifying the robustness of the framework of the MIL-53(AlCr) support in the reaction.

To explore the extendibility of the Ru–B/MIL-53(AlCr) catalyst in the hydrogenation of other aromatic compounds, methyl group(s)-substituted benzene derivatives (toluene, three xylene isomers, and mesitylene) were used as the substrates under the same reaction conditions as those of benzene, which gave the corresponding saturated cycloparaffin as the only detectable product. Table 2 shows that this catalyst was also active in the hydrogenation of the benzene derivatives under mild reaction conditions. The r_0 and TOF values ranked as toluene > *o*-xylene > *m*-xylene > *p*-xylene > mesitylene, which is consistent with the order found for toluene, *o*-xylene, and mesitylene on NFS-Ru(0).[6] The reactivities of the methyl-substituted benzene derivatives in general decreased with the increase in the number of methyl groups, which may be explained by the electronic effect of the methyl group.[6] As an electron-donating group, the more the methyl substituents, the higher the density of the π-electron cloud on the phenyl ring is, hence the benzene derivative with more methyl groups becomes more stable.

Conclusions

The MIL-53(Al)-, MIL-53(Cr)-, and MIL-53(AlCr)-supported Ru–B catalysts were prepared by the facile wetness impregnation–chemical reduction method that enabled high metal dispersion while the framework of the MIL-53 MOFs remained intact. In liquid-phase hydrogenation of benzene to cyclohexane under mild reaction conditions of 30 °C and 1.0 MPa of H_2, they exhibited higher activities than previously reported supported Ru catalysts. Among them, the Ru–B/MIL-53(AlCr) catalyst displayed the highest TOF of 6.4 s^{-1}. Moreover, it was stable in repeated catalytic runs and showed excellent activities in catalysing the hydrogenation of toluene, *o*-xylene, *m*-xylene, *p*-xylene, and mesitylene as well. The present work demonstrates that a highly active and reusable aromatic hydrogenation catalyst adaptable to mild reaction conditions can be

designed by choosing suitable MOFs as the supports for the Ru–B NPs. By optimizing the Al/Cr ratio and the reaction variables, it is promising to enhance further the catalytic performance of the Ru–B/MIL-53(AlCr) catalyst.

Acknowledgements

Notes and references

1 K. Weissermel and H. J. Arpe, *Industrial Organic Chemistry*, Wiley-VCH, Weinheim, 2003, ch. 10.

2 J. Zhang and M. H. Liu, *Chem. Ind. Eng. Prog.*, 2009, **28**, 634–638.

3 A. Stanislaus and B. H. Cooper, *Catal. Rev.: Sci. Eng.*, 1994, **36**, 75–123.

4 S. K. Sharma, K. B. Sidhpuria and R. V. Jasra, *J. Mol. Catal. A: Chem.*, 2011, **335**, 65–70.

5 R. L. Augustine, *Heterogeneous Catalysis for the Synthetic Chemistry*, Marcel Dekker, New York, 1996.

6 M. Zahmakıran, Y. Tonbul and S. Özkar, *J. Am. Chem. Soc.*, 2010, **132**, 6541–6549.

7 Y. Ma, Y. Huang, Y. Cheng, L. Wang and X. Li, *Appl. Catal., A*, 2014, **484**, 154–160.

8 A. Corma, H. García and F. X. L. i. Xamena, *Chem. Rev.*, 2010, **110**, 4606–4655.

9 K. Manna, T. Zhang, M. Carboni, C. W. Abney and W. B. Lin, *J. Am. Chem. Soc.*, 2014, **136**, 13182–13185.

10 J. An, S. J. Geib and N. L. Rosi, *J. Am. Chem. Soc.*, 2009, **131**, 8376–8377.

11 J. R. Li, R. J. Kuppler and H. C. Zhou, *Chem. Soc. Rev.*, 2009, **38**, 1477–1504.

12 Y. Peng, V. Krungleviciute, I. Eryazici, J. T. Hupp, O. K. Farha and T. Yildirim, *J. Am. Chem. Soc.*, 2013, **135**, 11887–11894.

13 F. Schröder, D. Esken, M. Cokoja, M. W. E. van den Berg, O. I. Lebedev, G. Van Tendeloo, B. Walaszek, G. Buntkowsky, H. Limbach, B. Chaudret and R. A. Fischer, *J. Am. Chem. Soc.*, 2008, **130**, 6119–6130.

14 Y. J. Zhao, J. L. Song, J. S. Li, J. L. Liu, T. B. Wu, P. Zhang and B. X. Han, *Green Chem.*, 2011, **13**, 2078–2082.

15 H. L. Liu, R. Q. Fang, Z. Li and Y. W. Li, *Chem. Eng. Sci.*, 2015, **122**, 350–359.

16 C. Serre, F. Millange, C. Thouvenot, M. Noguès, G. Marsolier, D. Louër and G. Férey, *J. Am. Chem. Soc.*, 2002, **124**, 13519–13521.

17 T. Loiseau, C. Serre, C. Huguenard, G. Fink, F. Taulelle, M. Henry, T. Bataille and G. Férey, *Chem. – Eur. J.*, 2004, **10**, 1373–1382.

18 S. H. Xie, M. H. Qiao, H. X. Li, W. J. Wang and J. F. Deng, *Appl. Catal., A*, 1999, **176**, 129–134.

19 Y. Pei, G. B. Zhou, N. Luan, B. N. Zong, M. H. Qiao and F. Tao, *Chem. Soc. Rev.*, 2012, **41**, 8140–8162.

20 Y. J. Zhao, J. L. Zhang, B. X. Han, J. L. Song, J. S. Li and Q. Wang, *Angew. Chem., Int. Ed.*, 2011, **50**, 636–639.

21 X. H. Tan, G. B. Zhou, R. F. Dou, Y. Pei, K. N. Fan, M. H. Qiao, B. Sun and B. N. Zong, *Acta Phys. Chim. Sin.*, 2014, **30**, 932–942.

22 T. B. Wu, P. Zhang, J. Ma, H. L. Fan, W. T. Wang, T. Jiang and B. X. Han, *Chin. J. Catal.*, 2013, **34**, 167–175.

23 Z. G. Sun, G. Li, L. P. Liu and H. O. Liu, *Catal. Commun.*, 2012, **27**, 200–205.

24 J. F. Moulder, W. F. Stickle, P. E. Sobol and K. D. Bomben, *Handbook of X-ray Photoelectron Spectroscopy*, ed. J. Chastain, Perkin-Elmer, Minnesota, 1992.

25 S. U. Nandanwar, M. Chakraborty, S. Mukhopadhyay and K. T. Shenoy, *React. Kinet., Mech. Catal.*, 2013, **108**, 473–489.